Bioinspired Modification of h-BN for High Thermal Conductive Composite Films with Aligned Structure

Heng Shen,[†,‡] Jing Guo,[†,‡] Hao Wang,[†,‡] Ning Zhao,*[,†] and Jian Xu*[,†]

[†]Beijing National Laboratory for Molecular Sciences, Laboratory of Polymer Physics and Chemistry, Institute of Chemistry, Chinese Academy of Sciences, Beijing 100190, China

[‡]University of Chinese Academy of Sciences, Beijing 100049, China

S *Supporting Information*

ABSTRACT: With the development of microelectronic technology, the demand of insulating electronic encapsulation materials with high thermal conductivity is ever growing and much attractive. Surface modification of chemical inert h-BN is yet a distressing issue which hinders its applications in thermal conductive composites. Here, dopamine chemistry has been used to achieve the facile surface modification of h-BN microplatelets by forming a polydopamine (PDA) shell on its surface. The successful and effective preparation of h-BN@PDA microplatelets has been confirmed by SEM, EDS, TEM, Raman spectroscopy, and TGA investigations. The PDA coating increases the dispersibility of the filler and enhances its interaction with PVA matrix as well. Based on the combination of surface modification and doctor blading, composite films with aligned h-BN@PDA are fabricated. The oriented fillers result in much higher in-plane thermal conductivities than the films with disordered structures produced by casting or using the pristine h-BN. The thermal conductivity is as high as 5.4 W m^{-1} K^{-1} at 10 vol % h-BN@PDA loading. The procedure is eco-friendly, easy handling, and suitable for the practical application in large scale.

KEYWORDS: *aligned structure, hexagonal boron nitride, polydopamine, thermal conductivity*
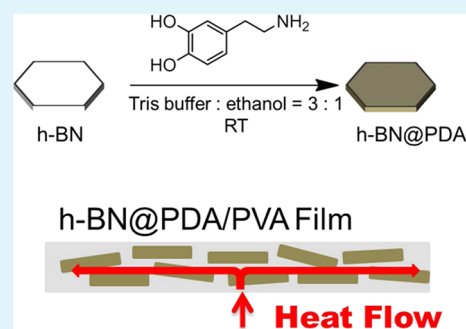
1. INTRODUCTION

Heat accumulation produced by the increasing power of electronics and industrial equipment may cause efficiency reduction and even equipment damage. To improve the heat dissipation, thermal interface materials have drawn increasing attention in recent years. Polymer composites consisting of a polymer matrix and heat conductive fillers with high thermal conductivity are usually the prior selection because of their easy process ability and low cost. Various low-cost ceramic fillers, including Al$_2$O$_3$,[1−3] Si$_3$N$_4$,[4,5] AlN,[6−9] SiC,[10,11] and so on, have been used as the heat conductive fillers. With the development of new carbon materials, carbon nanotubes[12−15] and graphene[16−22] have also been applied in fabricating high thermal conductive composites due to their super high thermal conductivity. However, the high cost and electrical conductivity of these carbon materials limit their applications, especially in electronic packaging where electrical insulation is required. Among different heat conductive fillers, hexagonal boron nitride (h-BN), also called white graphite due to a similar hexagonal structure to graphite, has received far more attention because of its unique advantages.[23−25] Different from graphite, h-BN is a semiconductor with a wide band gap making it electrical insulating, and compared to traditional ceramic fillers mentioned above, h-BN has a lower density and a higher thermal conductivity. Therefore, h-BN has great potential application in thermal conductive composites.

The interface thermal resistance between fillers and matrixes will hinder the enhancement of thermal conductivity. Surface modification of inorganic fillers has been demonstrated to be an efficient way to improve the miscibility and affinity with organic polymers, which is of benefit to increase the thermal conductivity of the composites.[8,26,27] However, due to the chemical inertness, surface modification of h-BN is troublesome. Functional molecules with conjugate structures are applied in modifying h-BN nanosheets though π−π interaction. Lewis acid−base complexation is used to modify h-BN as well. Lin et al.[28] mixed h-BN powder with either octadecylamine (ODA) or an amine-terminated oligomeric polyethylene glycol (PEG) to obtain ODA- or PEG-functionalized h-BN though the interaction between the B atoms and the amino groups. Yu et al.[27] functionalized h-BN nanoplatelets with γ-aminopropyl-triethoxysilane and then linked a hyperbranched aromatic polyamide to improve the interaction between h-BN and epoxy matrix. Hydroxyl groups can be introduced on the surface of h-BN by treatment with hydrogen peroxide at high temperature.[29] Nevertheless, long time and high energy cost make these methods low efficiency, and the reagents used may harm the environment. Therefore, it is desirable to develop a

convenient and eco-friendly strategy to functionalize the boron nitride.

Besides the surface modification of the fillers, the orientation of the anisotropic fillers is another important issue to reach a high thermal conductivity. In general, utilizing the anisotropic materials to obtain aligned structure can lead to superior properties in mechanical property,[30,31] electrical conductivity,[32−36] thermal conductivity,[15,29,37−46] and so on. Efforts have been contributed to fabricate aligned structure in composites with anisotropic thermal conductive fillers such as carbon nanotubes,[15,43] graphene,[45,46] carbon fibers,[44] BN nanotubes,[37] and h-BN platelets[29,38−42] via different strategies including electrospinning,[37] chemical vapor deposition,[15] electrostatic flocking,[44] stretching,[39] induction by magnetic field,[38,40,41,46] and doctor blading.[29,42] Among these methods, doctor blading is a promising way to be applied in practical production due to its easy operation, no need for special equipment, and large scale production.

In our research, dopamine chemistry was applied to functionalize the commercial h-BN powder. Due to the similar chemical structure with 3,4-dihydroxy-L-phenylalanine which is responsible for the strong and universal adhesion of mussel, dopamine is widely used in surface functionalization recently.[47−50] It is easily oxidized to self-polymerize into polydopamine (PDA) coating on almost all kinds of substrates in alkaline aqueous solution.[51] Carbon nanotubes,[52−55] graphene,[56−61] fibers,[62,63] clay,[64] and other particles[65,66] have been modified via dopamine chemistry and applied in fabricating high performance composites. This bioinspired method is regarded as an easy and green surface modification method owing to its room temperature reaction and no harmful solvents involved. Herein, h-BN microplatelets were modified by PDA, and the resultant powder could be easily dispersed in water and in PVA matrix as well. Doctor blading was carried out to fabricate h-BN/PVA composite films with an aligned structure, which was identified to have a higher in-plane thermal conductivity. The result indicates the promising prospect in industry production.

2. EXPERIMENTAL SECTION

2.1. Materials. The h-BN powder (∼10 μm, purity >99.5%) was provided by Dandong Rijin Science and Technology Co., Ltd. Dopamine hydrochloride was purchased from Alfa. PVA-124, tris(hydroxymethyl) aminomethane (Tris), hydrochloric acid (∼38 wt % aqueous solution), and absolute ethanol (AR) were purchased from Beijing Chemical Reagent Company. For all experiments, deionized water was used.

2.2. Surface Modification of h-BN. The h-BN powder of 2 g was dispersed in the mixed solution of 300 mL of Tris-buffer solution (10 mM, pH 8.5) and 100 mL of ethanol, and then 800 mg of dopamine hydrochloride was added, and the mixture was stirred for 6 h at room temperature. After the reaction, the modified h-BN powder, denoted as h-BN@PDA, was centrifuged and washed by deionized water and ethanol for several times before being dried at 60 °C.

2.3. Preparation of Composite Films. A certain amount of h-BN@PDA powder was dispersed in 18 g of deionized water by ultrasonication for 30 min. Then 2 g of PVA was added, and the mixture was stirred at 90 °C for 3 h to form a 10 wt % PVA aqueous solution containing different contents of h-BN@PDA. Composite films with orientated structure were prepared by using a doctor blade with a height of 1 mm at a speed of 5 cm/s. In the control experiment, composite films were fabricated by casting the solution into a Teflon mold. Films were left to dry at 40 °C for 24 h and then further dried in a vacuum oven at 60 °C for another 24 h under reduced pressure.

2.4. Characterization. Scanning electron microscope (SEM) studies were performed on a JSM-7500F (JEOL, Japan) at an accelerating voltage of 5 kV. The SEM-EDS test was carried out at 15 kV. Transmission electron microscope (TEM) studies were conducted on a JEM-2100F (JEOL, Japan) at an accelerating voltage of 200 kV. Thermogravimetric analysis was performed on Pyris 1 TGA (PerkinElmer, America) at a heating rate of 10 °C/min from 50 to 700 °C in an air stream with a flow rate of 20 mL/min. The Raman spectra were obtained on a Fourier transform Raman spectrometer RFS 100/S (Bruker, Germany) with an excitation wavelength at 1064 nm. Water contact angles were characterized using a KRÜSS DSA 100 by a sessile drop method. Water droplets of 5 μL were used, and the data were the average of five measurements at different places on the surface. Powder X-ray diffraction (XRD) patterns were taken on a Empyrean X-ray diffractometer (PANalytical, Netherlands) using Cu Kα radiation. The in-plane thermal diffusivity (α) of the composite film was detected by using a laser-flash diffusivity instrument LFA 447 (NETZSCH, Germany). The specimens were 25 mm in diameter and around 100 μm in thickness, spray-coated with a thin layer of fine graphite powder at both sides. The specific heat (c) was investigated by differential scanning calorimetry (DSC) Q2000 (TA Instruments, America) at a heating rate of 10 °C/min. The densities (ρ) of PVA, h-BN, and h-BN@PDA were measured by using an automatic density analyzer ULTRAPYC 1200e (Quantachrome Instruments, America). The densities and specific heats of the composite films were estimated according to the simple mixing role: composite = ν_{PVA} × PVA + ν_{filler} × filler, where ν denotes volume fractions. The thermal diffusivities, densities and specific heats were all characterized at 30 °C.

The in-plane thermal conductivities were calculated from the equation: $\lambda(T) = \alpha(T)\, \rho(T)\, c(T)$. The densities of h-BN and h-BN@PDA were 2.11 and 2.18 g cm^{-3}, and the specific heats were 0.95 and 0.91 J g^{-1} K^{-1}, respectively. The densities and specific heats of pristine h-BN and h-BN@PDA did not show obvious change because only a very thin PDA layer formed after the surface modification. The density and specific heat of the PVA matrix were 1.31 g cm^{-3} and 1.60 J g^{-1} K^{-1}.

3. RESULTS AND DISCUSSION

3.1. Surface Modification of h-BN. The procedure for fabrication of h-BN@PDA is shown in Scheme 1. Because of

Scheme 1. Schematic Illustration of the Surface Modification of h-BN Microplatelets by Dopamine Chemistry
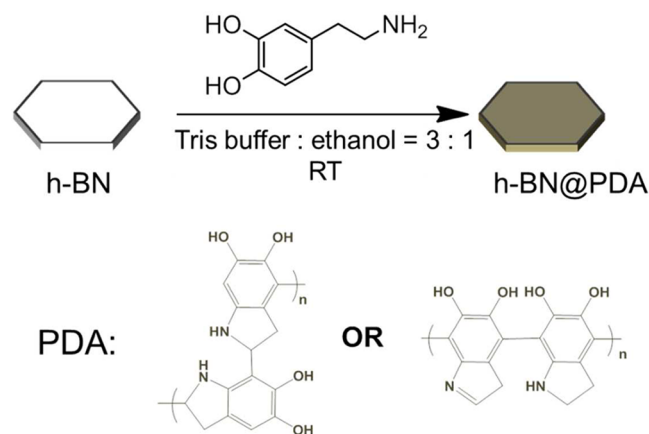
the hydrophobicity of h-BN powder, ethanol was added into Tris-buffer solution to improve the dispersibility of h-BN. On the other hand, ethanol can slow down the polymerization rate of dopamine in Tris-buffer solution,[67] preventing the aggregation of h-BN microplatelets with each other.

Due to the formation of a thin layer of PDA on the h-BN surface, the color of the powder turned from white to gray after
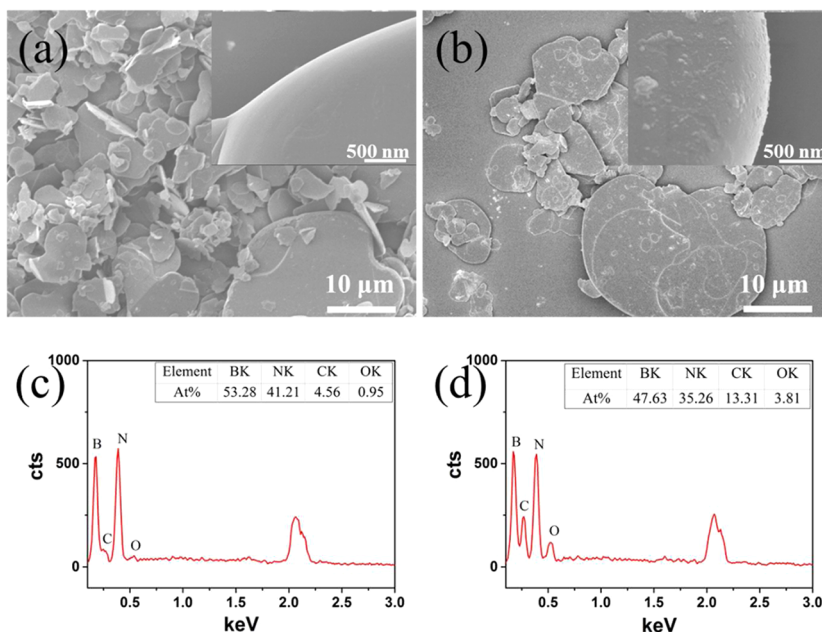
Figure 1. SEM images of (a) pristine h-BN and (b) h-BN@PDA, and EDS results of (c) pristine h-BN and (d) h-BN@PDA. Insets in (a) and (b) are the enlarged view.

modification. The surface topography and the element composition of h-BN platelets before and after modification were investigated by SEM and EDS, as shown in Figure 1. The h-BN microplatelets show a well flaked structure and smooth surface (Figure 1a) and have an average lateral size of about 10.4 ± 5.0 μm (Supporting Information (SI), Figure S1). After modification, aggregation of the microplatelets cannot be observed, and from a higher magnification it can be seen that the surface of the platelets became rougher and small particles appeared on the surface of h-BN@PDA (Figure 1b). This is because PDA particles are inevitably formed during the modification.[68] The EDS result shows that pristine h-BN is composed of B, N, C, and O elements. The small amount of C and O elements may be introduced by impurities from synthetic process. In comparison, the noteworthy increase of the C and O after modification demonstrates the deposition of PDA on the h-BN surface. TEM images in Figure 2 clearly reveal a thin layer of PDA with a thickness of about 4 nm deposited on h-BN.

The surface chemical compositions were further confirmed by Raman spectra (Figure 3). Raman shift at 1364 cm^{-1} was the characteristic peak of hexagonal BN ascribed to the high frequency intra layer E2g vibration mode. A new peak at 1530
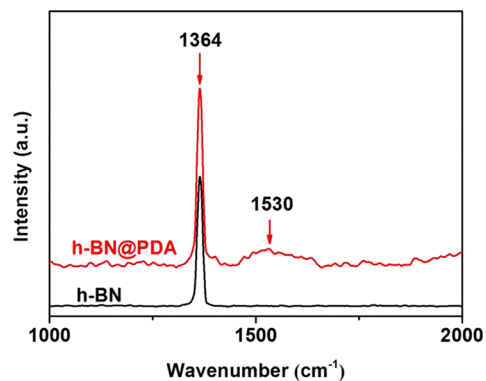

Figure 3. Raman spectra of h-BN and h-BN@PDA.

cm^{-1} appeared after modification, which was ascribed to the deformation of catechol moiety of PDA.[69] The thermogravimetric analyses disclosed that the content of PDA deposited on the h-BN surface was about 3.5% (Figure 4). This content could be adjusted by tuning the initial dosage of dopamine and reaction time.[70]
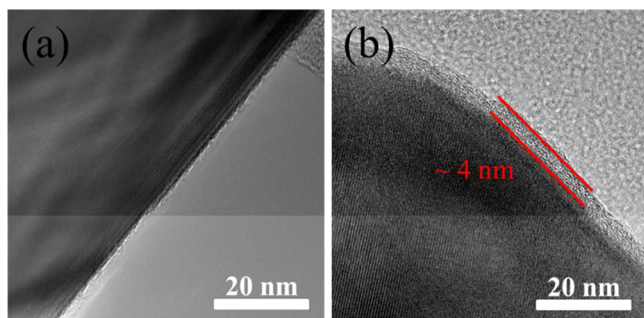

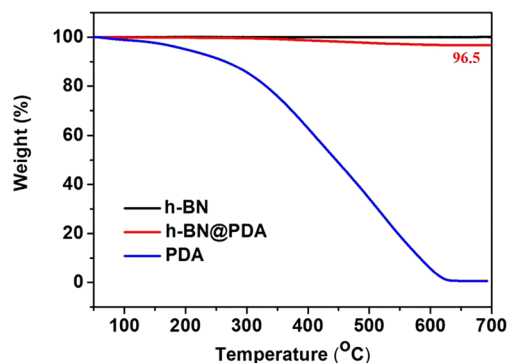**Figure 2.** TEM images of (a) pristine h-BN and (b) h-BN@PDA microplatelets.

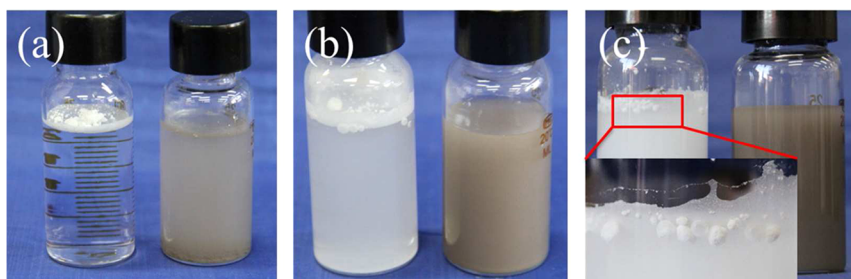**Figure 4.** TGA curves of h-BN, h-BN@PDA, and PDA.

Figure 5. Photographs showing the difference of the dispersibility of the microplatelets in water. (a) h-BN (left) and h-BN@PDA (right) platelets were just added into water, (b) after 10 min of ultrasonication, and (C) after intensely shaking and another 10 min of ultrasonication.

It is believed that substrates having conjugate structure such as graphene, carbon nanotubes, and BN nanotubes show strong π−π interaction with PDA[55,60,69] Therefore, the similar hexagonal conjugate structure of h-BN microplatelets can be easily and efficiently modified by means of dopamine chemistry. The phenolic hydroxyl and amine groups of PDA made h-BN@PDA more hydrophilic and apt to be dispersible in water. Figure 5 shows the dispersibility of the microplatelets in water. Due to the hydrophobicity of h-BN,[71] the pristine platelets floated on the water surface when they were added into water. Conversely, the h-BN@PDA platelets sank to the bottom quickly (Figure 5a). After ultrasonication (300W, 40 Hz) for 10 min, the h-BN@PDA dispersed in water completely while most of the h-BN remained floating on the water surface (Figure 5b), and these h-BN aggregations could still be observed on the water surface after further intensely shaking and another 10 min of ultrasonication (Figure 5c). The conspicuous differences in dispersibility in water between pristine and modified h-BN evidenced the efficiency of PDA coating. The characterization above suggested the successful deposition of PDA on the h-BN surface.

3.2. Composite Film with Aligned Structure. Composite film of h-BN@PDA in PVA with an aligned structure has been obtained by doctor blading. As revealed by the cross section SEM images of the composite films with 20 vol % fillers, h-BN@PDA dispersed well in the PVA matrix (Figure 6a). The shear force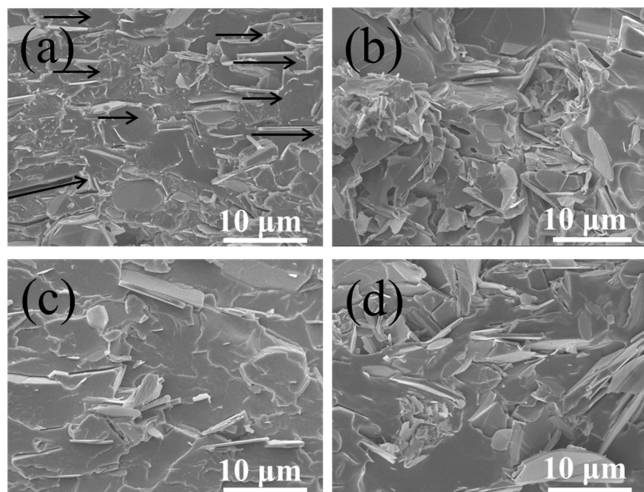 introduced by doctor blading resulted in good orientation of h-BN@PDA along the force direction (arrows in Figure 6a). Different from the doctor blading, the casting method only lead to a more irregular arrangement of h-BN@PDA (Figure 6c) because of the lack of extra orienting force. It is worth noting that h-BN@PDA fillers were still well dispersed in PVA without obvious aggregation, implying the importance of surface modification. The hydroxyl as well as amino groups of PDA increased the affinity between h-BN@PDA fillers and the PVA matrix through hydrogen bond.[72] In contrast, the pristine h-BN fillers aggregated in PVA and arranged disorderly, no matter the film was obtained by casting or doctor blading. This can be attributed to the hydrophobic nature of h-BN making the fillers easier to aggregate in hydrophilic PVA matrix (Figure 6b,d). The aggregation was so strong that the shear force of doctor blading could not lead to a well aligned structure (Figure 6b). In addition, the wettability of the composite films changed. A typical photograph of the h-BN/PVA and h-BN@PDA/PVA composite films was shown in Figure S2 in the SI. Compared to the h-BN@PDA/PVA film with a smooth surface, small protuberances were observed on the h-BN/PVA film. The protuberances could be ascribed to the aggregations of h-BN platelets. Because of the increased hydrophilicity of the fillers after PDA modification and the enhanced dispersibility in PVA as a result, the water contact angle of h-BN@PDA/PVA was only $54 \pm 4°$, compared to the $71 \pm 5°$ for the h-BN/PVA film.

The XRD detection of the composite films provides additional support for the formation of the alignment structure. The ratio of the intensity of the peaks at approximately 26.9° and 41.6°, which are assigned to the (002) and (100) crystallographic planes of hexagonal BN, respectively, represents the orientation degree of h-BN platelets.[29,42] Figure 7 gives the XRD patterns of the different composite films

Figure 6. Cross-section SEM images of the composite films fabricated by doctor blading with 20 vol % of (a) h-BN@PDA and (b) h-BN; and prepared by casting with 20 vol % of (c) h-BN@PDA and (d) h-BN.
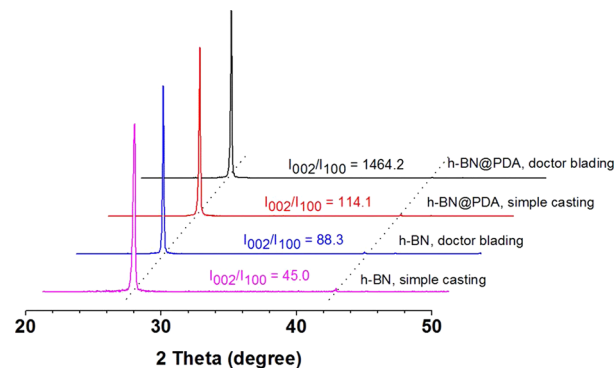

Figure 7. XRD patterns of different composite films containing 20 vol % fillers.

containing 20 vol % fillers. It reveals that, although the composite film was prepared by simple casting with pristine h-BN fillers, the intensity of (002) was much larger than that of (100), since the large ratio of the lateral size to thickness of the microplatelets preferred the fillers to arrange along the horizontal direction spontaneously. Doctor blading only promoted the alignment of h-BN platelets a little due to the intensive aggregation of h-BN. After the PDA modification, however, the orientation degree of h-BN@PDA/PVA by doctor blading obviously increased over that of the film prepared by casting.

Similar variation tendency for the orientation degree of the composite films with 10 and 30 vol % fillers were shown in Figure S3 to S6 in the SI. These results further confirm that the modification by means of dopamine chemistry greatly improves the dispersibility of the fillers in the PVA matrix, and a well aligned structure can be obtained in the composite films by the combination with doctor blading method. The XRD results are in agreement with SEM investigation, and can be also used to explain the difference in the thermal conductivity of the various composite films mentioned in the following section.

3.3. Thermal Conductivities of Composite Films.

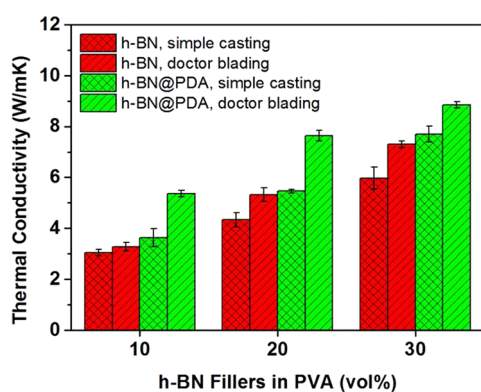Figure 8 shows the in-plane thermal conductivities of the

Figure 8. In-plane thermal conductivities of composite films prepared.

composite films prepared. The results demonstrate that thermal conductivity increased with the fraction of the fillers. Moreover, for the same filler concentration it can be seen: (1) using h-BN@PDA always lead to a higher thermal conductivity than pristine h-BN; (2) doctor blading resulted in a higher thermal conductivity than casting. The differences can be ascribed to the improved dispersibility of the filler after surface modification and the orientation effect of doctor blading as well. The results are in agreement with the SEM and XRD investigations, suggesting that the aligned structure could efficiently form thermal conductive pathways along the oriented direction. In addition, the increased affinity between h-BN@PDA fillers and PVA matrix through hydrogen bond also decreased the interfacial thermal resistance, which is another contribution for the high thermal conductivity. From Figure 8 we can see the conductivity of the composite films containing h-BN@PDA from casting is always higher than that of the film containing pristine h-BN prepared from doctor blading. The XRD results also reveal that the former has a good dispersibility. This may be because a uniform dispersion of the fillers rooted from PDA modification is more effective to get a higher conductivity than the blading method.

Table 1 summarizes the physical properties of h-BN@PDA/PVA composite films fabricated by doctor blading. The aligned

Table 1. Physical Properties of Composite Films Fabricated by Doctor Blading with Different Volume Fractions of h-BN@PDA Fillers

vol. fraction (vol %)	density (g cm^{-3})	specific heat (J g^{-1} K^{-1})	thermal diffusivity (mm^2 s^{-1})	thermal conductivity (W m^{-1} K^{-1})
0	1.31	1.60	0.13	0.3
10	1.40	1.53	2.50	5.4
20	1.48	1.46	3.54	7.6
30	1.57	1.39	4.05	8.8

structure of h-BN@PDA remarkably enhanced the in-plane thermal conductivity, which reached 5.4, 7.6, and 8.8 W m^{-1} K^{-1} for 10, 20, and 30 vol % fillers, respectively. It is seen that the thermal conductivity was approximately 63%, 44%, and 21% higher than that of h-BN/PVA fabricated by doctor blading method. In the case of cast composites, however, the corresponding increase of thermal conductivity was only 20%, 25%, and 25%. It can be explained according to the orientation degree given by XRD investigation. For the casting method, the orientation degree of h-BN@PDA/PVA films enhanced closely at each content of fillers compared to h-BN/PVA films. Therefore, the thermal conductivities increased similarly. However, for the doctor blading method, the I_{002}/I_{100} of h-BN@PDA/PVA films increased from 85.8 to 1526.7 and 88.3 to 1464.2 for 10 and 20 vol % fillers, while for the 30 vol % composite film, the I_{002}/I_{100} just increased from 66.9 to 527.4. Therefore, the thermal conductivity of the 30 vol % composite film enhanced less. The SEM and XRD investigations both show that the arrangement of the microplatelets of 30 vol % was less well orientated. It is speculated that, with the increase of the filler contents, the viscosity increased correspondingly, which hindered the alignment of the microplatelets.[41] The relative disordered structure of h-BN@PDA fillers decreased the efficiency of heat transmission along the in-plane direction, thus a small increase in thermal conductivity resulted. Although doctor blading is not as excellent as other methods such as LbL to produce perfectly aligned structures, it is still efficient to enhance the in-plane thermal conductivities of composite films.

Compared to the previously reported results with the similar aligned structure, our method is preferable owing to the larger microplatelets used and the effective surface modification of h-BN. For example, Xie et al.[29] fabricated the composite films with the thermal conductivity of about 4.5 W m^{-1} K^{-1} at 30 wt % h-BN. Ahn et al.[42] obtained the composite films with the thermal diffusivities of 0.90, 1.35, and 2.48 mm^2 s^{-1} at 10, 20, and 30 vol % h-BN, respectively. Because the thermal conductivity of h-BN increases with the decreasing of its thickness, the thermal diffusivity reached 9 mm^2 s^{-1} at only 15 vol % h-BN nanosheets obtained by Song and co-workers.[39] However, the exfoliation of h-BN nanosheets from microplatelets required huge energy and time. This work provided an optimized alternative of thermal conductivity and the fabrication process.

4. CONCLUSIONS

Bioinspired dopamine chemistry was applied to modify the chemically inert h-BN microplatelets. Compared with other reported methods which usually require strong base, oxidant,

special organic solvents, and other harsh experimental conditions, this facile and green approach at room temperature performs as a preferential alternative. After modification, the dispersibility of h-BN microplatelets in the PVA matrix was prominently improved. Composite films with an aligned structure of the fillers, which formed efficient thermal pathways to get a higher thermal conductivity at the same filler content, could be easily obtained by doctor blading method. This is beneficial to reduce the amount of fillers for fabricating lightweight and high thermal conductive composites. The modification and fabrication methods are facile handling, eco-friendly, and suitable for large scale production. Furthermore, postmodification can be carried out easily taking advantage of the reactivity of PDA,[73,74] which may adjust the surface condition of h-BN further and broaden its applications thereby.

■ ASSOCIATED CONTENT

Ⓢ Supporting Information

Size distribution of h-BN, photos and water contact angles of the composite films containing 20 vol % filler prepared by doctor blading, SEM images, and XRD of composite films with 10 and 30 vol % fillers. This material is available free of charge via the Internet at http://pubs.acs.org.

■ AUTHOR INFORMATION

Corresponding Authors
*E-mail: zhaoning@iccas.ac.cn.
*E-mail: jxu@iccas.ac.cn.

Notes
The authors declare no competing financial interest.

■ ACKNOWLEDGMENTS

■ REFERENCES

(1) Zhang, S.; Ke, Y.; Cao, X.; Ma, Y.; Wang, F. Effect of Al_2O_3 Fibers on the Thermal Conductivity and Mechanical Properties of High Density Polyethylene with the Absence and Presence of Compatibilizer. *J. Appl. Polym. Sci.* **2011**, *124*, 4874–4881.

(2) Zhou, Y.; Wang, H.; Xiang, F.; Zhang, H.; Yu, K.; Chen, L. A Poly(Vinylidene Fluoride) Composite with Added Self-Passivated Microaluminum and Nanoaluminum Particles for Enhanced Thermal Conductivity. *Appl. Phys. Lett.* **2011**, *98*, 182906.

(3) Wu, X.; Jiang, P.; Zhou, Y.; Yu, J.; Zhang, F.; Dong, L.; Yin, Y. Influence of Alumina Content and Thermal Treatment on the Thermal Conductivity of UPE/Al_2O_3 Composite. *J. Appl. Polym. Sci.* **2014**, *131*, 40528.

(4) Cui, W.; Zhu, Y.; Yuan, X.; Chen, K.; Kang, F. Gel-Cast-Foam-Assisted Combustion Synthesis of Elongated β-Si_3N_4 Crystals and Their Effects on Improving the Thermal Conductivity of Silicone Composites. *J. Alloys Compd.* **2012**, *540*, 165–169.

(5) Kusunose, T.; Yagi, T.; Firoz, S. H.; Sekino, T. Fabrication of Epoxy/Silicon Nitride Nanowire Composites and Evaluation of Their Thermal Conductivity. *J. Mater. Chem. A* **2013**, *1*, 3440–3445.

(6) Wang, J.; Yi, X.-S. Preparation and the Properties of PMR-Type Polyimide Composites with Aluminum Nitride. *J. Appl. Polym. Sci.* **2003**, *89*, 3913–3917.

(7) Shi, Z.; Radwan, M.; Kirihara, S.; Miyamoto, Y.; Jin, Z. Enhanced Thermal Conductivity of Polymer Composites Filled with Three-Dimensional Brushlike AlN Nanowhiskers. *Appl. Phys. Lett.* **2009**, *95*, 224104.

(8) Huang, X.; Iizuka, T.; Jiang, P.; Ohki, Y.; Tanaka, T. Role of Interface on the Thermal Conductivity of Highly Filled Dielectric Epoxy/AlN Composites. *J. Phys. Chem. C* **2012**, *116*, 13629–13639.

(9) Zhou, Y.; Wang, H.; Wang, L.; Yu, K.; Lin, Z.; He, L.; Bai, Y. Fabrication and Characterization of Aluminum Nitride Polymer Matrix Composites with High Thermal Conductivity and Low Dielectric Constant for Electronic Packaging. *Mater. Sci. Eng., B* **2012**, *177*, 892–896.

(10) Li, Y.; Huang, X.; Hu, Z.; Jiang, P.; Li, S.; Tanaka, T. Large Dielectric Constant and High Thermal Conductivity in Poly-(Vinylidene Fluoride)/Barium Titanate/Silicon Carbide Three-Phase Nanocomposites. *ACS Appl. Mater. Interfaces* **2011**, *3*, 4396–4403.

(11) Cao, J. P.; Zhao, X.; Zhao, J.; Zha, J. W.; Hu, G. H.; Dang, Z. M. Improved Thermal Conductivity and Flame Retardancy in Poly-styrene/Poly(Vinylidene Fluoride) Blends by Controlling Selective Localization and Surface Modification of SiC Nanoparticles. *ACS Appl. Mater. Interfaces* **2013**, *5*, 6915–6924.

(12) Bozlar, M.; He, D.; Bai, J.; Chalopin, Y.; Mingo, N.; Volz, S. Carbon Nanotube Microarchitectures for Enhanced Thermal Conduction at Ultralow Mass Fraction in Polymer Composites. *Adv. Mater.* **2010**, *22*, 1654–1658.

(13) Chen, H.; Chen, M.; Di, J.; Xu, G.; Li, H.; Li, Q. Architecting Three-Dimensional Networks in Carbon Nanotube Buckypapers for Thermal Interface Materials. *J. Phys. Chem. C* **2012**, *116*, 3903–3909.

(14) Cui, W.; Du, F.; Zhao, J.; Zhang, W.; Yang, Y.; Xie, X.; Mai, Y.-W. Improving Thermal Conductivity While Retaining High Electrical Resistivity of Epoxy Composites by Incorporating Silica-Coated Multi-Walled Carbon Nanotubes. *Carbon* **2011**, *49*, 495–500.

(15) Wang, M.; Chen, H.; Lin, W.; Li, Z.; Li, Q.; Chen, M.; Meng, F.; Xing, Y.; Yao, Y.; Wong, C. P.; Li, Q. Crack-Free and Scalable Transfer of Carbon Nanotube Arrays into Flexible and Highly Thermal Conductive Composite Film. *ACS Appl. Mater. Interfaces* **2014**, *6*, 539–544.

(16) Huang, X.; Zhi, C.; Jiang, P. Toward Effective Synergetic Effects from Graphene Nanoplatelets and Carbon Nanotubes on Thermal Conductivity of Ultrahigh Volume Fraction Nanocarbon Epoxy Composites. *J. Phys. Chem. C* **2012**, *116*, 23812–23820.

(17) Shahil, K. M.; Balandin, A. A. Graphene-Multilayer Graphene Nanocomposites as Highly Efficient Thermal Interface Materials. *Nano Lett.* **2012**, *12*, 861–867.

(18) Araby, S.; Zhang, L.; Kuan, H.-C.; Dai, J.-B.; Majewski, P.; Ma, J. A Novel Approach to Electrically and Thermally Conductive Elastomers Using Graphene. *Polymer* **2013**, *54*, 3663–3670.

(19) Song, S. H.; Park, K. H.; Kim, B. H.; Choi, Y. W.; Jun, G. H.; Lee, D. J.; Kong, B. S.; Paik, K. W.; Jeon, S. Enhanced Thermal Conductivity of Epoxy-Graphene Composites by Using Non-Oxidized Graphene Flakes with Non-Covalent Functionalization. *Adv. Mater.* **2013**, *25*, 732–737.

(20) Kong, Q.-Q.; Liu, Z.; Gao, J.-G.; Chen, C.-M.; Zhang, Q.; Zhou, G.; Tao, Z.-C.; Zhang, X.-H.; Wang, M.-Z.; Li, F.; Cai, R. Hierarchical Graphene-Carbon Fiber Composite Paper as a Flexible Lateral Heat Spreader. *Adv. Funct. Mater.* **2014**, *24*, 4222–4228.

(21) Shen, B.; Zhai, W.; Zheng, W. Ultrathin Flexible Graphene Film: An Excellent Thermal Conducting Material with Efficient EMI Shielding. *Adv. Funct. Mater.* **2014**, *24*, 4542–4548.

(22) Teng, C.-C.; Ma, C.-C. M.; Lu, C.-H.; Yang, S.-Y.; Lee, S.-H.; Hsiao, M.-C.; Yen, M.-Y.; Chiou, K.-C.; Lee, T.-M. Thermal Conductivity and Structure of Non-Covalent Functionalized Graphene/Epoxy Composites. *Carbon* **2011**, *49*, 5107–5116.

(23) Lin, Y.; Connell, J. W. Advances in 2d Boron Nitride Nanostructures: Nanosheets, Nanoribbons, Nanomeshes, and Hybrids with Graphene. *Nanoscale* **2012**, *4*, 6908–6939.

(24) Miro, P.; Audiffred, M.; Heine, T. An Atlas of Two-Dimensional Materials. *Chem. Soc. Rev.* **2014**, *43*, 6537–6554.

(25) Pakdel, A.; Bando, Y.; Golberg, D. Nano Boron Nitride Flatland. *Chem. Soc. Rev.* **2014**, *43*, 934–959.

(26) Sato, K.; Horibe, H.; Shirai, T.; Hotta, Y.; Nakano, H.; Nagai, H.; Mitsuishi, K.; Watari, K. Thermally Conductive Composite Films

of Hexagonal Boron Nitride and Polyimide with Affinity-Enhanced Interfaces. *J. Mater. Chem.* **2010**, *20*, 2749−2752.

(27) Yu, J.; Huang, X.; Wu, C.; Wu, X.; Wang, G.; Jiang, P. Interfacial Modification of Boron Nitride Nanoplatelets for Epoxy Composites with Improved Thermal Properties. *Polymer* **2012**, *53*, 471−480.

(28) Lin, Y.; V. Williams, T.; W. Connell, J. Soluble, Exfoliated Hexagonal Boron Nitride Nanosheets. *J. Phys. Chem. Lett.* **2010**, *1*, 277−283.

(29) Xie, B.-H.; Huang, X.; Zhang, G.-J. High Thermal Conductive Polyvinyl Alcohol Composites with Hexagonal Boron Nitride Microplatelets as Fillers. *Compos. Sci. Technol.* **2013**, *85*, 98−103.

(30) Wang, J.; Cheng, Q.; Tang, Z. Layered Nanocomposites Inspired by the Structure and Mechanical Properties of Nacre. *Chem. Soc. Rev.* **2012**, *41*, 1111−1129.

(31) Yao, H. B.; Ge, J.; Mao, L. B.; Yan, Y. X.; Yu, S. H. 25th Anniversary Article: Artificial Carbonate Nanocrystals and Layered Structural Nanocomposites Inspired by Nacre: Synthesis, Fabrication and Applications. *Adv. Mater.* **2014**, *26*, 163−188.

(32) Lin, X.; Shen, X.; Zheng, Q.; Yousefi, N.; Ye, L.; Mai, Y.-W.; Kim, J.-K. Fabrication of Highly-Aligned, Conductive, and Strong Graphene Papers Using Ultralarge Graphene Oxide Sheets. *ACS Nano* **2012**, *6*, 10708−10719.

(33) Yousefi, N.; Gudarzi, M. M.; Zheng, Q.; Aboutalebi, S. H.; Sharif, F.; Kim, J.-K. Self-Alignment and High Electrical Conductivity of Ultralarge Graphene Oxide-Polyurethane Nanocomposites. *J. Mater. Chem.* **2012**, *22*, 12709−12717.

(34) Chen, G.; N. Futaba, D.; Kimura, H.; Sakurai, S.; Yumura, M.; Hata, K. Absence of an Ideal Single-Walled Carbon Nanotube Forest Structure for Thermal and Electrical Conductivities. *ACS Nano* **2013**, *7*, 10218−10224.

(35) Souier, T.; Maragliano, C.; Stefancich, M.; Chiesa, M. How to Achieve High Electrical Conductivity in Aligned Carbon Nanotube Polymer Composites. *Carbon* **2013**, *64*, 150−157.

(36) Ahadian, S.; Ramon-Azcon, J.; Estili, M.; Liang, X.; Ostrovidov, S.; Shiku, H.; Ramalingam, M.; Nakajima, K.; Sakka, Y.; Bae, H.; Matsue, T.; Khademhosseini, A. Hybrid Hydrogels Containing Vertically Aligned Carbon Nanotubes with Anisotropic Electrical Conductivity for Muscle Myofiber Fabrication. *Sci. Rep.* **2014**, *4*, 4271.

(37) Terao, T.; Zhi, C.; Bando, Y.; Mitome, M.; Tang, C.; Golberg, D. Alignment of Boron Nitride Nanotubes in Polymeric Composite Films for Thermal Conductivity Improvement. *J. Phys. Chem. C* **2010**, *114*, 4340−4344.

(38) Cho, H.-B.; Tokoi, Y.; Tanaka, S.; Suematsu, H.; Suzuki, T.; Jiang, W.; Niihara, K.; Nakayama, T. Modification of BN Nanosheets and Their Thermal Conducting Properties in Nanocomposite Film with Polysiloxane According to the Orientation of BN. *Compos. Sci. Technol.* **2011**, *71*, 1046−1052.

(39) Song, W. L.; Wang, P.; Cao, L.; Anderson, A.; Meziani, M. J.; Farr, A. J.; Sun, Y. P. Polymer/Boron Nitride Nanocomposite Materials for Superior Thermal Transport Performance. *Angew. Chem., Int. Ed.* **2012**, *51*, 6498−6501.

(40) Lim, H. S.; Oh, J. W.; Kim, S. Y.; Yoo, M.-J.; Park, S.-D.; Lee, W. S. Anisotropically Alignable Magnetic Boron Nitride Platelets Decorated with Iron Oxide Nanoparticles. *Chem. Mater.* **2013**, *25*, 3315−3319.

(41) Lin, Z.; Liu, Y.; Raghavan, S.; Moon, K. S.; Sitaraman, S. K.; Wong, C. P. Magnetic Alignment of Hexagonal Boron Nitride Platelets in Polymer Matrix: Toward High Performance Anisotropic Polymer Composites for Electronic Encapsulation. *ACS Appl. Mater. Interfaces* **2013**, *5*, 7633−7640.

(42) Ahn, H. J.; Eoh, Y. J.; Park, S. D.; Kim, E. S. Thermal Conductivity of Polymer Composites with Oriented Boron Nitride. *Thermochim. Acta* **2014**, *590*, 138−144.

(43) Koo, B.; Goli, P.; V. Sumant, A.; Claro, P.; Rajh, T.; S. Johnson, C.; A. Balandin, A.; V. Shevchenko, E. Toward Lithium Ion Batteries with Enhanced Thermal Conductivity. *ACS Nano* **2014**, *8*, 7202−7207.

(44) Uetani, K.; Ata, S.; Tomonoh, S.; Yamada, T.; Yumura, M.; Hata, K. Elastomeric Thermal Interface Materials with High through-Plane Thermal Conductivity from Carbon Fiber Fillers Vertically Aligned by Electrostatic Flocking. *Adv. Mater.* **2014**, DOI: 10.1002/adma.201401736.

(45) Xin, G.; Sun, H.; Hu, T.; Fard, H. R.; Sun, X.; Koratkar, N.; Borca-Tasciuc, T.; Lian, J. Large-Area Freestanding Graphene Paper for Superior Thermal Management. *Adv. Mater.* **2014**, *26*, 4521−4526.

(46) Yan, H.; Tang, Y.; Long, W.; Li, Y. Enhanced Thermal Conductivity in Polymer Composites with Aligned Graphene Nanosheets. *J. Mater. Sci.* **2014**, *49*, 5256−5264.

(47) Lynge, M. E.; van der Westen, R.; Postma, A.; Stadler, B. Polydopamine−a Nature-Inspired Polymer Coating for Biomedical Science. *Nanoscale* **2011**, *3*, 4916−4928.

(48) Ye, Q.; Zhou, F.; Liu, W. Bioinspired Catecholic Chemistry for Surface Modification. *Chem. Soc. Rev.* **2011**, *40*, 4244−4258.

(49) Sedo, J.; Saiz-Poseu, J.; Busque, F.; Ruiz-Molina, D. Catechol-Based Biomimetic Functional Materials. *Adv. Mater.* **2013**, *25*, 653−701.

(50) Liu, Y.; Ai, K.; Lu, L. Polydopamine and Its Derivative Materials: Synthesis and Promising Applications in Energy, Environmental, and Biomedical Fields. *Chem. Rev.* **2014**, *114*, 5057−5115.

(51) Lee, H.; Dellatore, S. M.; Miller, W. M.; Messersmith, P. B. Mussel-Inspired Surface Chemistry for Multifunctional Coatings. *Science* **2007**, *318*, 426−430.

(52) Fei, B.; Qian, B.; Yang, Z.; Wang, R.; Liu, W. C.; Mak, C. L.; Xin, J. H. Coating Carbon Nanotubes by Spontaneous Oxidative Polymerization of Dopamine. *Carbon* **2008**, *46*, 1795−1797.

(53) Hu, H.; Yu, B.; Ye, Q.; Gu, Y.; Zhou, F. Modification of Carbon Nanotubes with a Nanothin Polydopamine Layer and Polydimethy-lamino-Ethyl Methacrylate Brushes. *Carbon* **2010**, *48*, 2347−2353.

(54) Yan, P.; Wang, J.; Wang, L.; Liu, B.; Lei, Z.; Yang, S. The in Vitro Biomineralization and Cytocompatibility of Polydopamine Coated Carbon Nanotubes. *Appl. Surf. Sci.* **2011**, *257*, 4849−4855.

(55) Shi, C.; Deng, C.; Zhang, X.; Yang, P. Synthesis of Highly Water-Dispersible Polydopamine-Modified Multiwalled Carbon Nanotubes for Matrix-Assisted Laser Desorption/Ionization Mass Spectrometry Analysis. *ACS Appl. Mater. Interfaces* **2013**, *5*, 7770−7776.

(56) Kang, S. M.; Park, S.; Kim, D.; Park, S. Y.; Ruoff, R. S.; Lee, H. Simultaneous Reduction and Surface Functionalization of Graphene Oxide by Mussel-Inspired Chemistry. *Adv. Funct. Mater.* **2011**, *21*, 108−112.

(57) Tian, Y.; Cao, Y.; Wang, Y.; Yang, W.; Feng, J. Realizing Ultrahigh Modulus and High Strength of Macroscopic Graphene Oxide Papers through Crosslinking of Mussel-Inspired Polymers. *Adv. Mater.* **2013**, *25*, 2980−2983.

(58) Zhang, Z.; Zhang, J.; Zhang, B.; Tang, J. Mussel-Inspired Functionalization of Graphene for Synthesizing Ag-Polydopamine-Graphene Nanosheets as Antibacterial Materials. *Nanoscale* **2013**, *5*, 118−123.

(59) Dong, Z.; Wang, D.; Liu, X.; Pei, X.; Chen, L.; Jin, J. Bio-Inspired Surface-Functionalization of Graphene Oxide for Adsorption of Organic Dyes and Heavy Metal Ions with Superhigh Capacity. *J. Mater. Chem. A* **2014**, *2*, 5034−5040.

(60) He, Y.; Wang, J.; Zhang, H.; Zhang, T.; Zhang, B.; Cao, S.; Liu, J. Polydopamine-Modified Graphene Oxide Nanocomposite Membrane for Proton Exchange Membrane Fuel Cell under Anhydrous Conditions. *J. Mater. Chem. A* **2014**, *2*, 9548−9558.

(61) Lee, T.; Jeon, E. K.; Kim, B.-S. Mussel-Inspired Nitrogen-Doped Graphene Nanosheet Supported Manganese Oxide Nanowires as Highly Efficient Electrocatalysts for Oxygen Reduction Reaction. *J. Mater. Chem. A* **2014**, *2*, 6167−6173.

(62) Wang, W.; Li, R.; Tian, M.; Liu, L.; Zou, H.; Zhao, X.; Zhang, L. Surface Silverized Meta-Aramid Fibers Prepared by Bio-Inspired Poly(Dopamine) Functionalization. *ACS Appl. Mater. Interfaces* **2013**, *5*, 2062−2069.

(63) Chen, S.; Cao, Y.; Feng, J. Polydopamine as an Efficient and Robust Platform to Functionalize Carbon Fiber for High-Performance Polymer Composites. *ACS Appl. Mater. Interfaces* **2014**, *6*, 349−356.

(64) Huang, S.; Yang, L.; Liu, M.; Phua, S. L.; Yee, W. A.; Liu, W.; Zhou, R.; Lu, X. Complexes of Polydopamine-Modified Clay and

Ferric Ions as the Framework for Pollutant-Absorbing Supramolecular Hydrogels. *Langmuir* **2013**, *29*, 1238−1244.

(65) Thakur, V. K.; Vennerberg, D.; Madbouly, S. A.; Kessler, M. R. Bio-Inspired Green Surface Functionalization of Pmma for Multifunctional Capacitors. *RSC Adv.* **2014**, *4*, 6677−6684.

(66) Thakur, V. K.; Vennerberg, D.; Kessler, M. R. Green Aqueous Surface Modification of Polypropylene for Novel Polymer Nanocomposites. *ACS Appl. Mater. Interfaces* **2014**, *6*, 9349−9356.

(67) Yan, J.; Yang, L.; Lin, M.-F.; Ma, J.; Lu, X.; Lee, P. S. Polydopamine Spheres as Active Templates for Convenient Synthesis of Various Nanostructures. *Small* **2013**, *9*, 596−603.

(68) Bernsmann, F.; Ponche, A.; Ringwald, C.; Hemmerle, J.; Raya, J.; Bechinger, B.; Voegel, J.-C.; Schaaf, P.; Ball, V. Characterization of Dopamine-Melanin Growth on Silicon Oxide. *J. Phys. Chem. C* **2009**, *113*, 8234−8242.

(69) Thakur, V. K.; Yan, J.; Lin, M.-F.; Zhi, C.; Golberg, D.; Bando, Y.; Sim, R.; Lee, P. S. Novel Polymer Nanocomposites from Bioinspired Green Aqueous Functionalization of BNNTs. *Polym. Chem.* **2012**, *3*, 962−969.

(70) Ball, V.; Frari, D. D.; Toniazzo, V.; Ruch, D. Kinetics of Polydopamine Film Deposition as a Function of pH and Dopamine Concentration: Insights in the Polydopamine Deposition Mechanism. *J. Colloid Interface Sci.* **2012**, *386*, 366−372.

(71) Lin, Y.; Williams, T. V.; Xu, T.-B.; Cao, W.; Elsayed-Ali, H. E.; Connell, J. W. Aqueous Dispersions of Few-Layered and Monolayered Hexagonal Boron Nitride Nanosheets from Sonication-Assisted Hydrolysis: Critical Role of Water. *J. Phys. Chem. C* **2011**, *115*, 2679−2685.

(72) Hwang, S.-H.; Kang, D.; S. Ruoff, R.; Shin, H. S.; Park, Y.-B. Poly(Vinyl Alcohol) Reinforced and Toughened with Poly-(Dopamine)-Treated Graphene Oxide, and Its Use for Humidity Sensing. *ACS Nano* **2014**, *8*, 6739−6747.

(73) Lee, H.; Rho, J.; Messersmith, P. B. Facile Conjugation of Biomolecules onto Surfaces via Mussel Adhesive Protein Inspired Coatings. *Adv. Mater.* **2009**, *21*, 431−434.

(74) Kang, S. M.; Hwang, N. S.; Yeom, J.; Park, S. Y.; Messersmith, P. B.; Choi, I. S.; Langer, R.; Anderson, D. G.; Lee, H. One-Step Multipurpose Surface Functionalization by Adhesive Catecholamine. *Adv. Funct. Mater.* **2012**, *22*, 2949−2955.